Atomic Structure of Antiphase Domain Boundaries of a Thin Al_2O_3 Film on NiAl(110)

M. Kulawik,* N. Nilius, H.-P. Rust, and H.-J. Freund

Fritz-Haber-Institut der Max-Planck-Gesellschaft, Faradayweg 4-6, D-14195 Berlin, Germany

(Received 15 July 2003; published 16 December 2003)

Line defects of a thin alumina film on NiAl(110) have been studied on the atomic level with scanning tunneling microscopy at 4 K. While boundaries between two reflection domains do not expose a characteristic structure, antiphase domain boundaries are well ordered. The latter boundaries result from the insertion of a row of O atoms, as atomically resolved images of the topmost oxygen layer show. The insertion occurs only in two of the three characteristic directions of the quasihexagonal O lattice. Depending on the direction, either straight or zigzagged boundaries form. An atomic characterization of line defects on the oxide surface is a first step to correlate their topographic structure and chemical activity.

DOI: 10.1103/PhysRevLett.91.256101 PACS numbers: 68.35.Dv, 68.35.Bs, 68.37.Ef

Alumina is one of the most frequently used oxide supports for transition metals in heterogeneous catalysis [1]. Despite the importantance of Al_2O_3, only little is known about its defect structure, which is believed to strongly influence the catalytic activity of the material. So far, defects on oxide surfaces have been experimentally studied only in a few cases. On $TiO_2(110)$, for instance, scanning tunneling microscopy (STM) gave evidence of oxygen vacancies and their decisive role in the dissociation of H_2O [2,3]. However, the knowledge of defects on catalytically relevant oxide surfaces has been mostly gained by a combination of experimental and theoretical work [4,5]. In this Letter, we present STM measurements of line defects in a thin Al_2O_3 film on NiAl(110), which is a well-established support in Al_2O_3-based model catalysts [6–8]. Previous experiments have shown that these dislocations strongly influence the nucleation and growth of metal clusters, such as Pd or Rh [9]. Though it has been possible to describe the atomic structure of the Pd clusters via STM [10], the microscopic structure of the underlying line defects has not yet been unraveled. However, their topographic and electronic structure is of fundamental interest since they influence the number density and the average size of the clusters. For the first time, atomically resolved STM images of antiphase domain boundaries (APDB) in Al_2O_3 on NiAl(110) are presented, allowing the structure determination of these dislocations in the topmost oxygen layer.

All STM images were taken in ultrahigh vacuum, using a home-built microscope [11] operated at 4 and 77 K, respectively. The clean NiAl(110) surface was obtained by repeated cycles of Ar^+ sputtering and annealing to 1000 °C. The quality of the surface was checked by LEED and STM. Afterwards, the thin oxide film was prepared by dosing 1200 L O_2 at 280 °C and subsequent annealing to 800 °C for about 5 min [12]. In order to fill open patches in the film, a second oxidation cycle was applied.

The thin alumina film on NiAl(110) has been characterized by various methods, such as LEED, ARUPS, ISS, XPS, HREELS, and STM [12–15]. First, a short summary of the most important features is given. The atomically flat film exhibits a thickness of approximately 5 Å, corresponding to two Al-O layers. Results from transmission electron microscopy (TEM) [16] and phonon spectra [12,14] point to a γ-like structure. However, other stackings, such as in κ alumina, are also discussed [17], and the thin nature of the film hampers the assignment to a specific alumina phase. Ion-scattering spectroscopy (ISS) revealed that the surface is oxygen terminated, with the oxygen ions forming a quasihexagonal lattice.

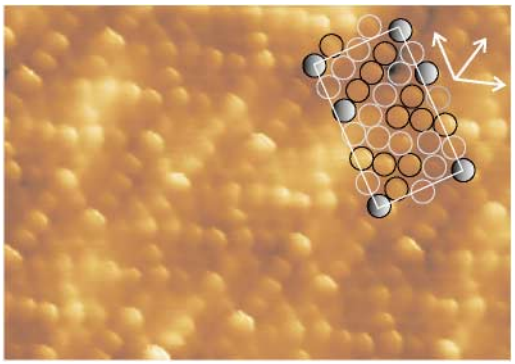

FIG. 1 (color online). Atomically resolved STM image of a thin Al_2O_3 film on NiAl(110), taken at ~4 K with V_S = 500 mV, I_T = 1 nA (58 Å × 40 Å). All atoms exhibit a quasihexagonal coordination, where the three characteristic directions are marked with arrows. The unit cell was determined from repetition of atoms. Here, gray-filled circles mark the most prominent atomic features, thus characterizing six positions of the cell. Furthermore, a zigzagged pattern is observed, where the atoms appear alternately larger and smaller. Differences in the apparent height are emphasized with black and gray circles, respectively.

 © 2003 The American Physical Society

In Fig. 1, an atomically resolved STM image of the alumina film is presented.

All atoms of the lattice show a quasihexagonal coordination as expected for close-packed oxygen layers in the Al_2O_3 film. The three directions determining this lattice are marked with arrows. The unit cell ($b_1 = 10.6$ Å, $b_2 = 17.9$ Å, $a = 88.6°$) can be easily assigned from repetition of atoms with similar size and brightness. For better visualization, atoms with the largest apparent height are marked with filled gray circles, defining six positions in the unit cell. The size and the orientation of the unit cell were confirmed by an autocorrelation function, which is a well-established tool for the determination of periodic structures in complex images. The assigned unit cell is in good agreement with previous results [15]. The observed symmetry suggests that mainly the topmost oxygen layer is imaged, while the contribution arising from the Al^{3+} sublattice is very small. In contrast to the first publication presenting atomically resolved images of the quasihexagonal oxygen lattice [15], the images here clearly reveal a zigzagged corrugation, where the atoms appear alternately smaller and bigger. In Fig. 1, this is illustrated for some atoms, which are marked with gray outlined (small atoms) and black outlined (big atoms) circles. Images exhibiting this corrugation have been obtained several times at different sample bias V_S. Therefore it is highly probable that the sensitivity to the outer orbitals of the terminating oxygen ions strongly depends on electronic tip properties. We assign the zigzag pattern mainly to a topographic effect where every second oxygen sticks out. Such a surface reconstruction would increase the distance between nearest oxygen neighbors and reduce the strain in the topmost oxygen layer. The O-O distance in the film (about 3 Å) is already slightly increased compared to typical values for bulk alumina (2.7 Å in γ-Al_2O_3) [18]. However, a careful theoretical study would be necessary to estimate the effect of the lower surface coordination and the role of the NiAl support.

Al_2O_3 grows on the metal substrate in two reflection domains, denoted A and B [Fig. 2(a)].

They are inclined by about 24° against the $[1\bar{1}0]$ direction of the NiAl(110). Whereas commensurate growth is observed along the $[1\bar{1}0]$ direction, growth is incommensurate along [001]. The existence of two reflection domains as well as the slight mismatch between the substrate and the film leads to a characteristic network of line defects. In addition, point defects were detected with a concentration of about 10^{13} cm^{-2} [9].

The network of dislocations becomes apparent in the STM image of Fig. 2(b). Two types of line defects can be distinguished on the alumina film: reflection domain boundaries separating the areas A and B and antiphase domain boundaries (APDB) between domains of equal orientation, i.e., A/A or B/B. The structure and the direction of the reflection domain boundaries are primarily determined by the growth of the domains A and B. They do not show local order and are not further discussed in this Letter. In contrast, APDB form very regularly with a mean distance of approximately 100 Å. They run along two well-defined directions in each domain, which is schematically shown in Fig. 2(a). When parallel to the b_1 vector of the Al_2O_3 unit cell, they appear as straight lines (IA and IB). In contrast, the thinner, zigzagged type

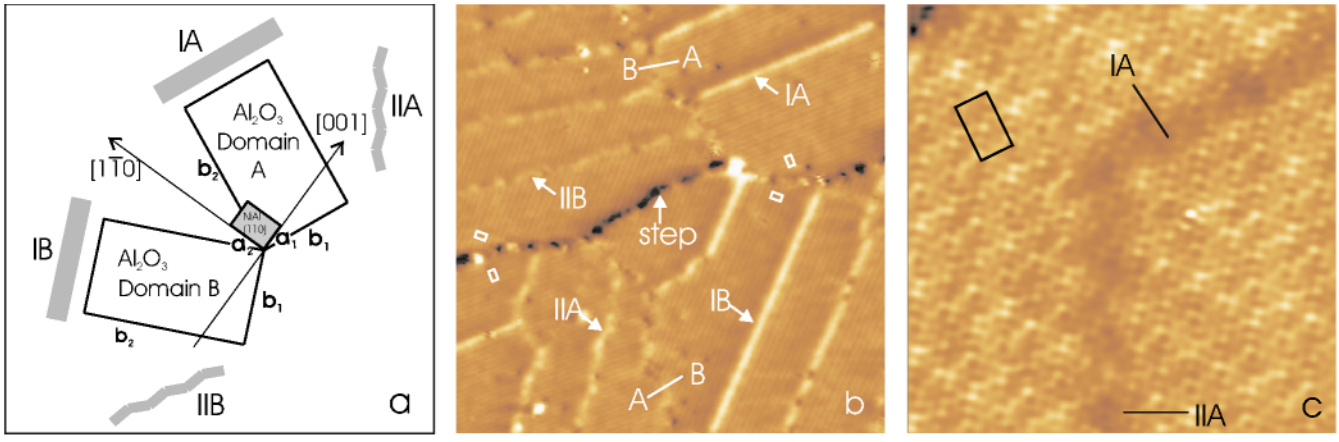

FIG. 2 (color online). (a) Dimension of the Al_2O_3 unit cell ($b_1 = 10.55$ Å, $b_2 = 17.89$ Å, $a = 88.6°$) and orientation with respect to the NiAl(110) substrate ($a_1 = 2.89$ Å, $a_2 = 4.08$ Å). The orientation and structure of the APDB is shown schematically (IA, IIA, IB, IIB). (b) Thin alumina film on NiAl(110), imaged at 77 K ($V_S = 4.5$ V, $I_T = 0.5$ nA, 378 Å × 378 Å). The z signal was differentiated, thus both terraces appear on the same height. The size and the orientation of the Al_2O_3 unit cell is marked with a white rectangle in each domain. APDB appear as bright lines, where a straight (IA and IB) and a zigzagged (IIA and IIB) type can be distinguished for each domain. In contrast to reflection domain boundaries (A-B), each of them runs along a characteristic direction. (c) STM image with higher resolution ($V_S = -2.0$ V, $I_T = 0.5$ nA, 129 Å × 129 Å) of a straight (IA) and a zigzagged (IIA) APDB in the A domain.

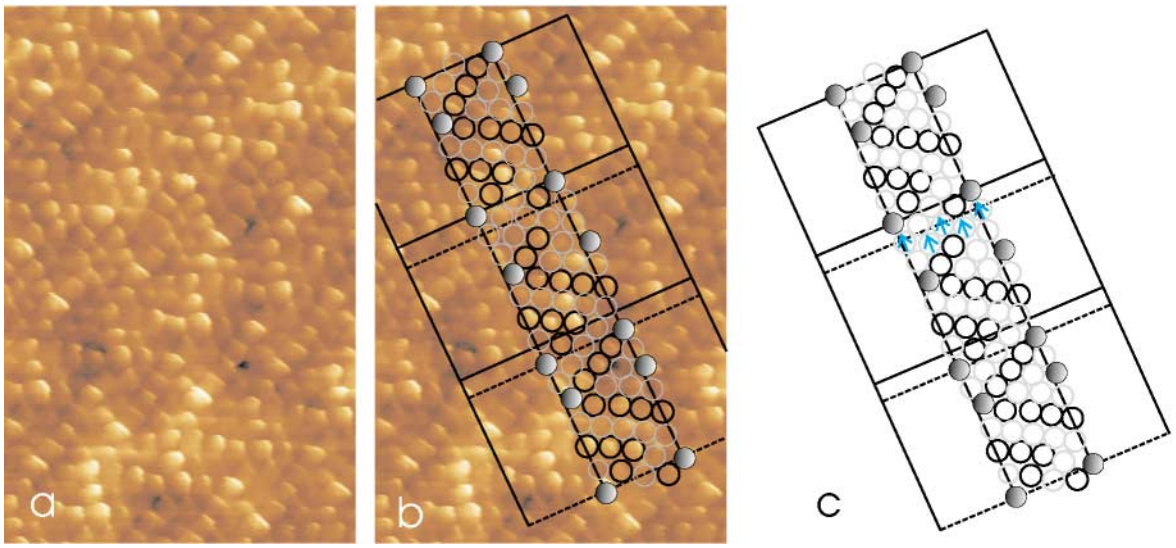

FIG. 3 (color). (a) Topmost layer of a straight boundary between two A domains (type IA), imaged with atomic resolution at ~4 K with $V_S = 200$ mV, $I_T = 0.6$ nA (46 Å × 70 Å). Part (b) displays the same image as (a), but additionally, the lattices on either side of the defect and the oxygen positions are marked; (c) shows the derived model for this APDB. The dislocation along b_1 is due to the insertion of oxygen along the arrows.

follows the diagonal of the unit cell (IIA and IIB). Figure 2(c) displays a high-resolution image of both a straight (IA) and a zigzagged boundary (IIA) in the A domain.

Although it has been possible to image each of the four APDB with atomic resolution, we concentrate in this paper only on the results for the domain A. In the B domain, the structures are identical (except from the orientation) as expected from the twofold symmetry of the alumina film with respect to the substrate. A high-resolution STM image of a straight APDB is shown in Fig. 3(a).

The boundary runs from the lower left to the upper right of the image. The unit cells on either side of the defect was determined as described above. In Fig. 3(b), the corresponding lattices are marked with straight and dotted lines, respectively. Based on this, a model of this boundary type is shown in Fig. 3(c). It turns out, that the

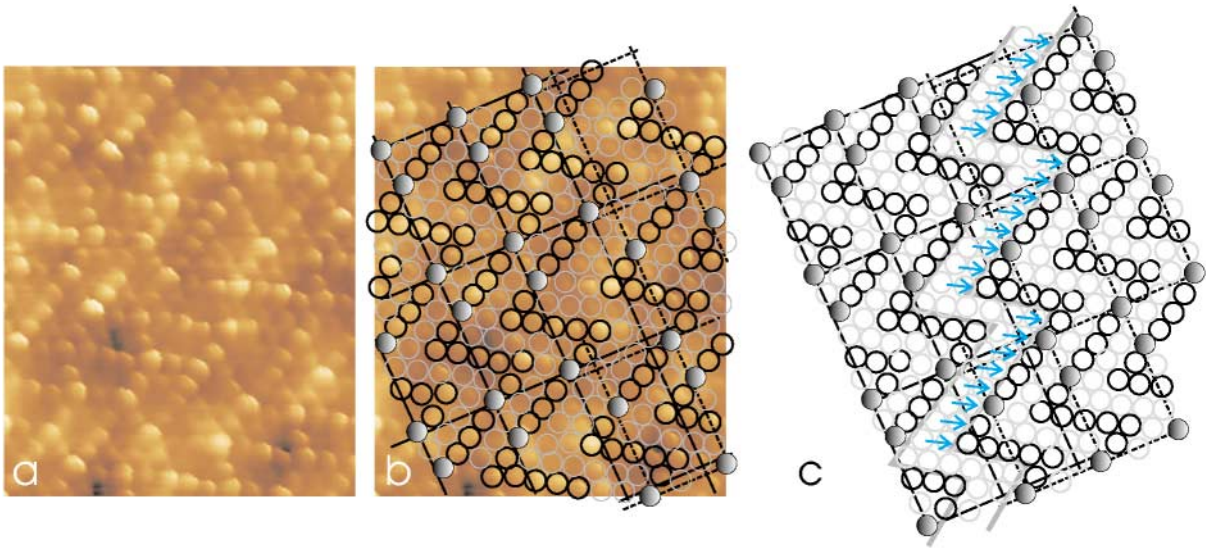

FIG. 4 (color). (a) Topmost layer of a zigzagged boundary between two A domains (type IIA), imaged with atomic resolution at 4 K with $V_S = 500$ mV, $I_T = 1$ nA (45 Å × 56 Å). (b) diplays the same image as (a) with lattices and oxygen positions drawn in. The resulting model is shown in (c), where blue arrows mark the inserted oxygen ions. The zigzagged boundary results from the insertion of an oxygen row orientated 60° to b_2, which jumps to the 4th next row every eight atoms.

lattice shift results from the insertion of a row of oxygen ions parallel to the b_1 vector of the Al_2O_3 unit cell, characterizing the macroscopic direction of this dislocation. The corresponding Burgers vector is orientated perpendicular to the inserted oxygen row, that is along the b_2 vector.

The microscopic structure of the zigzagged antiphase domain boundaries is quite different, as can be seen in Fig. 4(a). Here, oxygen ions are inserted in an angle of 60° with respect to b_2 and follow a different direction of the quasihexagonal oxygen lattice. Every eight atoms, the inserted line jumps to the 4th next oxygen row. The resulting rippled structure follows the reconstruction of the topmost oxygen layer as described above. Thus, the microscopic direction of this line defect differs from its macroscopic orientation, which is well aligned to the diagonal of the Al_2O_3 unit cell. In Fig. 4(b), the atom positions and the unit cells are marked for either side of the domain boundary. An atomic model for the zigzagged dislocation is shown in Fig. 4(c).

Both the straight and the zigzagged dislocation are characterized by the insertion of an oxygen row along one direction of the quasihexagonal lattice. The corresponding Burgers vectors are marked with blue arrows in Figs. 3(c) and 4(c), respectively. One might expect yet another type of APDB where ions are inserted along the third vector of the quasihexagonal oxygen lattice. The resulting line defect would be orientated perpendicular to this direction, hence almost parallel to the $[1\bar{1}0]$ direction of the NiAl(110). However, this was not observed. Apparently, such a dislocation is not effective to reduce the strain in the Al_2O_3 unit cell. The direction of maximum strain can therefore be assumed to run along the $[1\bar{1}0]$ direction, which is also the direction of commensurate growth. Thus, both the straight and the zigzagged APDB have a large component compensating the strain, because they are inclined to the $[1\bar{1}0]$ direction by 67° and 55°, respectively. The existence of two very different types of dislocations might be due to the atomic arrangement in the alumina film. We suppose that the exact preparation conditions are decisive for the frequency of occurrence of the different APDB to compensate the strain. Step edges might also play a crucial role for the growth and hence for the favored type of APDB appearing for strain compensation.

In conclusion, STM was used to determine for the first time the atomic structure of antiphase domain boundaries in the topmost oxygen layer of a thin Al_2O_3 film on NiAl(110). APDB result from the insertion of an oxygen row but do not induce changes in the geometric height with respect to the surrounding oxide domains. The apparent corrugation of APDB on Al_2O_3 in STM images at certain bias voltages [Ref. [13] and Fig. 2(b)] must therefore arise from electronis properties of these dislocations. In order to understand the preferential cluster nucleation on APDB, it is thus necessary to characterize their electronic structure, which is the aim of further experiments.

M. K. thanks the Studienstiftung des deutschen Volkes for support.

*Electronic address: kulawik@fhi-berlin.mpg.de

[1] *Handbook of Heterogeneous Catalysis*, edited by G. Ertl, H. Knözinger, and J. Weitkamp (VCH, Weinheim, 1997).
[2] R. Schaub *et al.*, Phys. Rev. Lett. **87**, 266104 (2001).
[3] R. Schaub *et al.*, Science **299**, 377 (2003).
[4] S. Abbet *et al.*, J. Am. Chem. Soc. **122**, 3453 (2000).
[5] S. Abbet, U. Heiz, H. Häkkinen, and U. Landman, Phys. Rev. Lett. **86**, 5950 (2001).
[6] C. R. Henry, Surf. Sci. Rep. **31**, 235 (1998).
[7] M. Bäumer and H.-J. Freund, Prog. Surf. Sci. **61**, 127 (1999).
[8] R. Franchy, Surf. Sci. Rep. **38**, 195 (2000).
[9] M. Frank and M. Bäumer, Phys. Chem. Chem. Phys. **2**, 3723 (2000).
[10] K. Højrup Hansen *et al.*, Phys. Rev. Lett. **83**, 4120 (1999).
[11] H.-P. Rust, J. Buisset, E. K. Schweizer, and L. Cramer, Rev. Sci. Instrum. **68**, 129 (1997).
[12] R. M. Jaeger *et al.*, Surf. Sci. **259**, 235 (1991).
[13] J. Libuda *et al.*, Surf. Sci. **318**, 61 (1994).
[14] M. Frank *et al.*, Surf. Sci. **492**, 270 (2001).
[15] G. Ceballos *et al.*, Chem. Phys. Lett. **359**, 41 (2002).
[16] M. Klimenkov, S. Nepijko, H. Kuhlenbeck, and H.-J. Freund, Surf. Sci. **385**, 66 (1997).
[17] D. R. Jennison and A. Bogicevic, Surf. Sci. **464**, 108 (2000).
[18] G. Gutiérrez, A. Taga, and B. Johansson, Phys. Rev. B **65**, 012101 (2001).